AIRBORNE DOPPLER NAVIGATION SYSTEM APPLICATION FOR MEASUREMENT OF THE WATER SURFACE BACKSCATTERING SIGNATURE

A. Nekrasov [a]

[a] Taganrog Institute of Technology, Southern Federal University, 347922 Taganrog, Russia
Interdepartmental Center of Research in Environmental Sciences, University of Bologna, 48123 Ravenna, Italy
alexei-nekrassov@mail.ru

KEY WORDS: Sea, Measurement, Navigation, Active, Algorithms, Radar, Systems

ABSTRACT:

A method for measuring the water surface backscattering signature using the airborne Doppler navigation system in addition to its standard navigational application is discussed. A case of an airplane circle flight measurement of the azimuth normalized radar cross section curve of the water surface is considered. This is done in the range of middle incidence angles by the Doppler navigation system. The system operates in the scatterometer mode and uses a fore-beam directed to the right side at a typical mounting angle in the vertical plane that is not so far from nadir at a straight flight. An algorithm for measuring the water surface backscattering signature is proposed.

1. INTRODUCTION

Many researchers have been investigating the microwave backscattering signatures of the sea and ocean surfaces (Carswell et al, 1994; Chelton and McCabe, 1985; Feindt et al, 1986; Hildebrand, 1994; Masuko et al, 1986; Melnik, 1980; Moore and Fung, 1979; Wismann, 1989). However, the mechanics of interactions between water surfaces and microwaves have not been well studied in detail.

The typical method for describing sea clutter is in the form of the normalized radar cross section (NRCS), the statistical distribution of the NRCS, the amplitude correlation and the spectral shape of the Doppler returns.

To describe the radar backscatter from the water surfaces, three major scattering models are used: the Kirchhoff or Physical Optics model, the composite-surface or two-scale model, and the Bragg model. The Kirchhoff model assumes a perfectly conducting surface (unless it is modified to include the Fresnel reflection coefficient) and applies from small to intermediate incidence angles without shadowing effects. Apart from the implicit dependence on the Fresnel coefficient, there is no polarization dependence. The two-scale model assumes that the radar backscatter arises from a large number of slightly rough ripples, distributed over the long ocean waves. It has polarization dependence. These two models are generally used to interpret the data acquired by the synthetic aperture radar and real aperture radar of a variety of sea/oceanic features, including swell waves and internal waves. The Bragg model applies only to the slightly rough surfaces under low wind conditions (it is often used to describe the scattering from ripples in the two-scale model). The Bragg model has been used to interpret the ocean currents by high-frequency Doppler radar measurements at large incidence angles (Ouchi, 2000).

To explain adequately the microwave scattering signature of the water surface and to apply its features to remote sensing, a set of experiments, namely, experimental verification of the combined frequency, azimuth and incidence angles, and wind speed variations of the NRCS are required (Masuko et al, 1986). For that study, a scatterometer, radar designed for measuring the surface scatter characteristics, is used.

Research on microwave backscatter by the water surface has shown that the use of a scatterometer also allows an estimation of near-surface wind speed and direction because the NRCS of the water surface depends on the wind speeds and directions. Based on experimental data and scattering theory, a significant number of empirical and theoretical backscatter models and algorithms for estimation of a near-surface wind vector from satellite and airplane has been developed (Long et al, 1996). It is also very important for safe landing of amphibian aircrafts on the water surface.

To study a microwave backscattering signature of the water surface from airplane, an airborne scatterometer is used. The measurements are typically performed at either a circle track flight using fixed fan-beam antenna or a rectilinear track flight using rotating antenna (Carswell et al, 1994; Masuko et al, 1986; Wismann, 1989). Unfortunately, a microwave narrow-beam antenna has considerable size at Ku-, X- and C-bands that makes its placing on a flying apparatus difficult. Therefore, a better way needs to be found.

At least two ways can be proposed. The first way is to apply the airborne scatterometers with wide-beam antennas as it can lead to the reduction in the antenna size. The second way is to use the modified conventional navigation instruments of a flying apparatus in a scatterometer mode that seems more preferable.

From that point of view, a promising navigation instrument is the Doppler navigation system (DNS). Previous research of the DNS has shown that it allows measurement of the wind vector over the water surface when it operates as a multi-beam scatterometer under the horizontal rectilinear flight of a flying apparatus (Nekrasov, 2005a; Nekrasov, 2005b). Now, a method to measure the water surface backscattering signature by the airborne DNS operating in the scatterometer mode at aircraft circle flight in addition to its standard navigation application is discussed in this paper.

2. DOPPLER NAVIGATION SYSTEM

DNS is the self-contained radar system that utilizes the Doppler effect (Doppler radar) for measuring the ground speed and drift angle of flying apparatus and accomplishes its dead-reckoning navigation (Sosnovskiy and Khaymovich, 1987).

The internationally authorized frequency band of 13.25 to 13.4 GHz has been allocated for airborne Doppler navigation radar. A center frequency of 13.325 GHz of the band corresponds to a wave length of 2.25 cm. This frequency represents a good compromise between too low a frequency, resulting in low-velocity sensitivity and large aircraft antenna size and beam widths, and too high a frequency, resulting in excessive absorption and backscattering effects of the atmosphere and precipitation. (Earlier Doppler radars operated in two somewhat lower frequency bands, i.e., centered at 8.8 and 9.8 GHz, respectively, but now these bands are no longer used for stand-alone Doppler radars.) (Kayton and Fried, 1997).

Measurement of the wind vector and drift angle of flying apparatus is based on change of a Doppler frequency of the signal reflected from the underlying surface, depending on a spatial position of an antenna beam. Usually, an antenna of the DNS has three beams (λ-configuration; beams 1, 2, and 3) or four beams (x-configuration; beams 1, 2, 3, and 4) located in space as represented in Figure 1. An effective antenna beamwidth is of 3° to 10° (Kolchinskiy et al, 1975). Power reasons (DNS should operates over water as well as over land) and sensitivity of the DNS to velocity influence a choice of a mounting angle of a beam axis in the vertical plane θ_0.

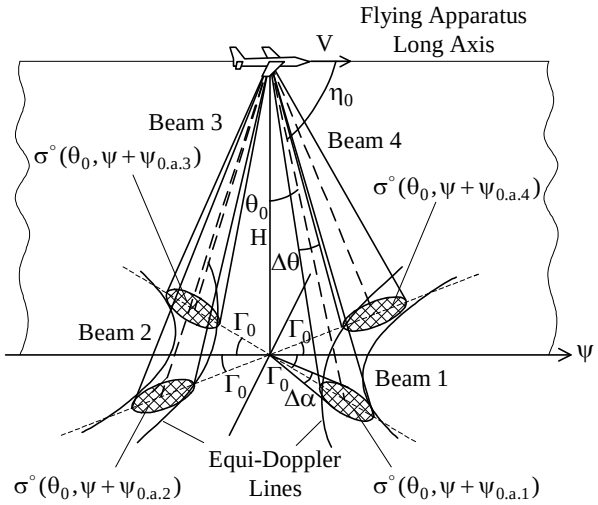

Figure 1. Typical spatial location of the DNS beams: λ-configuration (beams 1, 2, and 3) and x-configuration (beams 1, 2, 3, and 4)

Figure 2 shows curves of the NRCS of underlying surface versus incidence angle for radar system operating in the frequency band (Ke-band) currently assigned to Doppler navigation radar (Kayton and Fried, 1997). It is seen from the curves that for most types of terrain the NRCS decreases slowly with increase of the beam incidence angle. However, for water surfaces, the NRCS falls radically as the incidence angle increases and assumes different values for different conditions of sea state or water roughness. For the typical Doppler-radar incidence angles of 15° to 30° (Kolchinskiy et al, 1975), the NRCS is considerably smaller for most sea states than for land and decreases markedly for the smoother sea state. Therefore, a conservative Doppler-radar design is based on an NRCS for the smoothest sea state over which the aircraft is expected to navigate. (Very smooth sea states are relatively rare).

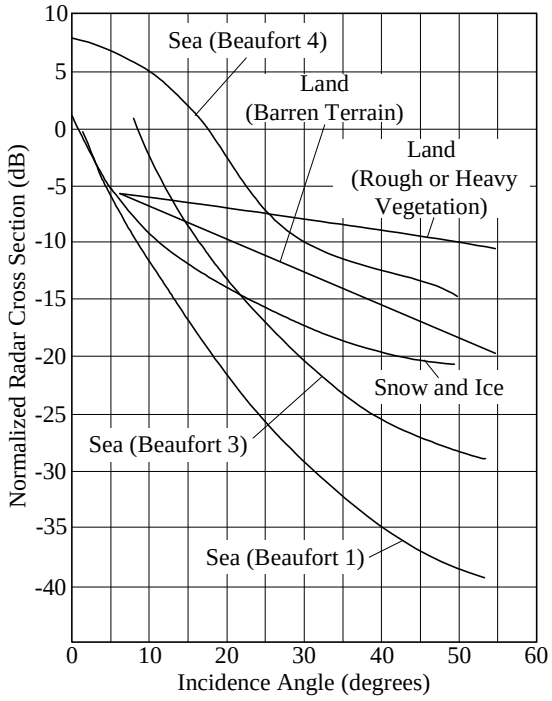

Figure 2. Backscattering cross section per unit surface area (NRCS) versus incidence angle for different terrains at Ke-band (Kayton and Fried, 1997)

There are two basic antenna system concepts used for drift angle measurement. These are the fixed-antenna system, which is used in most modern systems, and the track-stabilized (roll-and-pitch-stabilized) antenna system. For physically roll-and-pitch-stabilized antenna systems, the value of an incidence angle remains essentially constant and equal to the chosen design value. For fixed-antenna system, a conservative design is based on the NRCS and range for the largest incidence angle that would be expected for the largest combination of pitch and roll angles of the aircraft (Kayton and Fried, 1997).

The choice of a mounting angle of a beam axis in the inclined plane η_0 (nominal angle between antenna longitudinal axis and central beam direction) represents a compromise between high sensitivity to velocity and over-water accuracy, which increases with smaller mounting angles of a beam axis in the inclined plane, and high signal return over water, which increases for larger mounting angles of a beam axis in the inclined plane. Most equipments use a mounting angle of a beam axis in the inclined plane of somewhere between 65° and 80° (Kayton and Fried, 1997). The choice of a mounting angle of a beam axis in the horizontal plane Γ_0 depends on the desired sensitivity to drift, which tends to increase with increasing that mounting angle. For the typical Doppler-radar, mounting angles of a beam axis in the horizontal plane are of 15° to 45° (Kolchinskiy et al, 1975).

The relationship among those mounting angles is (Kayton and Fried, 1997)

$$\cos\eta_0 = \cos\Gamma_0 \cos\theta_0 \quad (1)$$

The mounting angle of a beam axis in the horizontal plane should satisfy the following condition $\Gamma_0 > \beta_{dr.\max}$, where $\beta_{dr.\max}$ is the maximum possible drift angle (Sosnovskiy and Khaymovich, 1987). The mounting angle of a beam axis in the inclined plane is defined by requirements to the width of a Doppler spectrum of the reflected signal Δf_D, which depends on the effective antenna beamwidth in the inclined plane $\theta_{a.incl}$; $\theta_{a.incl} \approx 5^\circ$ for DNS. The relative width of a Doppler spectrum $\Delta f_D / F_D$ is given by (Davydov et al, 1977)

$$\frac{\Delta f_D}{F_D} = \frac{\theta_{a.incl}}{\sqrt{2}} \tan\eta_0 \quad (2)$$

where F_D = Doppler frequency, $F_D = \frac{2V_g}{\lambda}\cos\eta_0$

V_g = aircraft velocity relative to the ground

λ = radar wavelength

To perform high accuracy measurements with the DNS, the following condition should be provided (Davydov et al, 1977)

$$\frac{\Delta f_D}{F_D} \le 0.1 \div 0.2 \quad (3)$$

Thus, from (2) and (3), the mounting angle of a beam axis in the inclined plane should satisfy the following condition

$$\eta_0 \le \arctan\left[(0.1 \div 0.2)\frac{\sqrt{2}}{\theta_{a.incl}}\right] \quad (4)$$

From (4), assuming that the effective antenna beamwidth in the inclined plane is typical and equal to 5°, the condition of choice the mounting angle of a beam axis in the inclined plane is

$$\eta_0 \le 58.3^\circ \div 72.2^\circ \quad (5)$$

Then, using (1), the areas of admissible mounting angles of beam axes could be obtained. Lower limits corresponding to the maximum admissible mounting angles of beam axis in the inclined plane and area of typical mounting angles of beam axes in the vertical and horizontal planes are represented in Figure 3. Trace 1 and trace 2 are the lower limits corresponding to the maximum admissible mounting angles of beam axis in the inclined plane of 58.3° (lower limit of high accuracy of measurement at $\Delta f_D / F_D = 0.1$) and 72.9° (lower limit of sufficient high accuracy of measurement at $\Delta f_D / F_D = 0.2$), respectively. A dash line displays the area of typical mounting angles of beam axes in the vertical and horizontal planes.

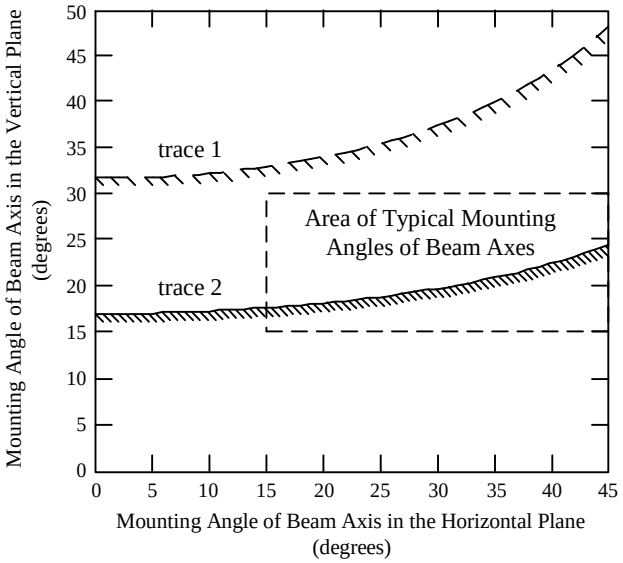

Figure 3. Lower limits corresponding to the maximum admissible mounting angles of beam axis in the inclined plane and area of typical mounting angles of beam axes in the vertical and horizontal planes: trace 1 is the lower limit corresponding to the maximum admissible mounting angle of beam axis in the inclined plane of 58.3° (lower limit of high accuracy of measurement at $\Delta f_D / F_D = 0.1$); trace 2 is the lower limit, which corresponds to the maximum admissible mounting angle of beam axis in the inclined plane of 72.9° (lower limit of sufficient high accuracy of measurement at $\Delta f_D / F_D = 0.2$); dash line is the contour of the area of typical mounting angles of beam axes in the vertical and horizontal planes

Figure 3 demonstrates that for typical mounting angles of beam axes, sufficient high accuracy of measurement by the DNS is provided for the most part of the area of typical mounting angles in the vertical and horizontal planes. The measurement accuracy rises with increase of the beam incidence angle in the vertical plane.

The DNS multi-beam antenna allows selecting a power backscattered by the underlying surface from different directions, namely from directions corresponding to the appropriate beam relative to the aircraft course ψ, e.g. $\psi_{0.a.1}$, $\psi_{0.a.2}$, $\psi_{0.a.3}$, and $\psi_{0.a.4}$ in Figure 1. Each beam provides angular resolutions in the azimuthal and vertical planes, $\Delta\alpha$ and $\Delta\theta$ respectively.

3. WATER SURFACE BACKSCATTERING SIGNATURE MEASUREMENT

As the azimuth NRCS curve can be obtained using the circle track flight for a scatterometer with an inclined one-beam fixed-position antenna (Masuko et al, 1986), one beam of the DNS operating in the scatterometer mode can be used.

Let the flying apparatus make a horizontal rectilinear flight with the speed V at some altitude H above the mean sea surface, and the DNS has a roll-and-pitch-stabilized antenna system. Then, the NRCS values obtained with beams 1, 2, 3, 4 would be $\sigma^\circ(\theta_0, \psi + \psi_{0.a.1})$, $\sigma^\circ(\theta_0, \psi + \psi_{0.a.2})$, $\sigma^\circ(\theta_0, \psi + \psi_{0.a.3})$, and $\sigma^\circ(\theta_0, \psi + \psi_{0.a.4})$ respectively.

Let the beam 1 be used to measure the water surface backscattering signature because both λ- and x-configured DNS have it. As a beam 1 axis is directed to the right side and its mounting angle in the vertical plane is not so far from nadir (at a straight flight), the circle flight with the left roll should be completed (Figure 4).

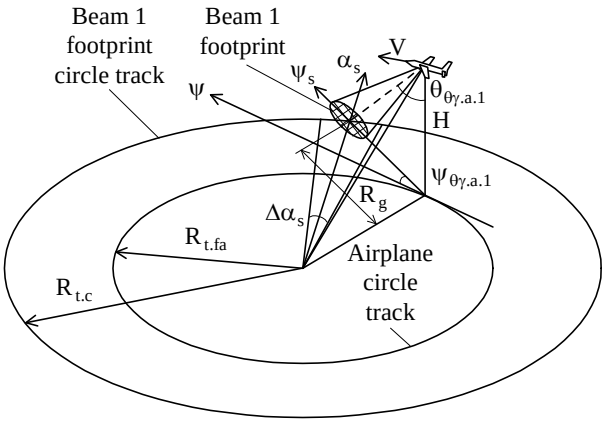

Figure 4. Circle flight geometry for measurement of the water surface backscattering signature

The DNS uses a fixed-antenna system (physically non-stabilized to the local horizontal), the flying apparatus makes the circle flight, and so the values of the incidence angle of the beam and the beam location in azimuthal plane are not equal to the chosen design values. An actual incidence angle of the beam 1 $\theta_{\theta\gamma.a.1}$ and its actual azimuth direction $\psi_{\theta\gamma.a.1}$ relative to the aircraft current course (aircraft ground track) are as following

$$\theta_{\theta\gamma.a.1} = \arctan\left(\sqrt{\tan^2(\arctan(\tan\theta_0 \sin\psi_{0.a.1}) + \gamma_{fa}) + \rightarrow} \rightarrow \overline{\tan^2(\arctan(\tan\theta_0 \cos\psi_{0.a.N}) + \theta_{fa})}\right) \quad (6)$$

$$\psi_{\theta\gamma.a.1} = \begin{cases} \arctan\left(\dfrac{\tan(\arctan(\tan\theta_0 \sin\psi_{0.a.1}) + \gamma_{fa})}{\tan(\arctan(\tan\theta_0 \cos\psi_{0.a.1}) + \theta_{fa})}\right) \\ \text{for } \tan(\arctan(\tan\theta_0 \cos\psi_{0.a.1}) + \theta_{fa}) \geq 0 \\ \pi + \\ \arctan\left(\dfrac{\tan(\arctan(\tan\theta_0 \sin\psi_{0.a.1}) + \gamma_{fa})}{\tan(\arctan(\tan\theta_0 \cos\psi_{0.a.1}) + \theta_{fa})}\right) \\ \text{for } \tan(\arctan(\tan\theta_0 \cos\psi_{0.a.1}) + \theta_{fa}) < 0 \end{cases} \quad (7)$$

where $\psi_{0.a.1}$ = azimuthal mounting angle of the beam 1 axis relative to the aircraft course ψ, $\psi_{0.a.1} = \Gamma_0$
γ_{fa} = roll angle of flying apparatus (right roll is positive)
θ_{fa} = pitch angle of flying apparatus (pull-up is positive)

Then, the current NRCS value obtained with the beam 1 is $\sigma^\circ(\theta_{\theta\gamma.a.1}, \psi + \psi_{\theta\gamma.a.1})$. The radius of the flying apparatus turn $R_{t.fa}$, the ground range R_g, and the radius of turn of the selected cell middle point $R_{t.c}$ are described by the following expressions obtained using the geometry of Figure 4

$$R_{t.fa} = \frac{V^2}{g \tan\gamma_{fa}} \quad (8)$$

$$R_g = \frac{H}{\tan\theta_{\theta\gamma.a.1}} \quad (9)$$

$$R_{t.c} = \sqrt{R_{t.fa}^2 + R_g^2 + 2R_{t.fa}R_g \sin\psi_{\theta\gamma.a.1}} \quad (10)$$

where g = acceleration of gravity, $g = 9.81$ m/s^2

The time of the airplane turn for 360° (360-degree turn) T_{360° is given by (Mamayev et al, 2002)

$$T_{360^\circ} = \frac{2\pi V}{g \tan\gamma_{fa}} \quad (11)$$

Usually, the 360-degree azimuth space is divided into 72 or 36 sectors under the circle NRCS measurement. The azimuth size of a sector observed is 5° or 10°, respectively. A middle azimuth of the sector is the azimuth of the sector observed. The azimuth size of a sector relative to the center point of circle of the airplane track is $\Delta\alpha_s$, and the middle azimuth of a sector is α_s. The NRCS samples obtained from the sector and averaged over all measurement values in that sector give the NRCS value $\sigma^\circ(\theta_{\theta\gamma.a.1}, \psi_s)$ corresponding to the real observation azimuth angle of the sector ψ_s that is

$$\psi_s = \psi_{\psi_s} + \psi_{\theta\gamma.a.1} \pm 360^\circ \quad (12)$$

where ψ_{ψ_s} = flying apparatus course corresponding to the real observation azimuth angle of the sector

Real observation azimuth angles of the sector beginning $\psi_{s.b}$ and of the sector ending $\psi_{s.e}$ are

$$\psi_{s.b} = \psi_s + \Delta\alpha_s / 2 \pm 360^\circ \quad (13)$$

$$\psi_{s.e} = \psi_s - \Delta\alpha_s / 2 \pm 360^\circ \quad (14)$$

The time of a sector view T_s and the number of samples N_s that can be obtained from the sector are represented by the following expressions

$$T_s = T_{360^\circ} \frac{\Delta\alpha_s}{360^\circ} \quad (15)$$

$$N_s = \frac{T_s V}{0.5a} \quad (16)$$

where a = antenna length in the direction of flight.

Thus, to obtain an azimuth NRCS curve of the water surface at middle incidence angles under flying apparatus circle flight by the DNS operating in the scatterometer mode and using a fore-beam directed to the right side at a typical mounting angle in the vertical plane that is not so far from nadir at a straight flight, the measurement should be perform in accordance with a scheme of Figure 5.

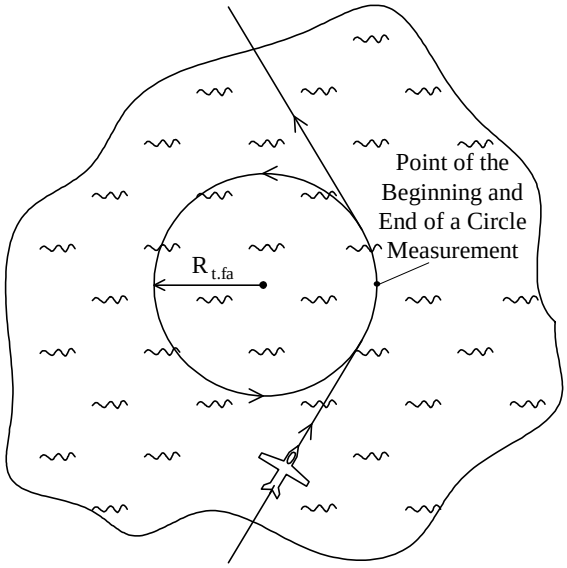

Figure 5. Scheme of a circle flight for measurement of the water surface backscattering signature

Measurement is started when a stable flight at the given altitude, speed of flight, roll and pitch has been established. Measurement is finished when the azimuth of the measurement beginning is reached. To obtain a greater number of NRCS samples for each sector observed several consecutive full circle turns for 360° may be done.

4. CONCLUSIONS

The study has shown that the airborne DNS operating in the scatterometer mode can be used for measuring the water surface backscattering signature in addition to its typical navigation application.

As the azimuth NRCS curve for a scatterometer with an inclined one-beam fixed-position antenna can be obtained using the circle track flight, one beam of the DNS can be used.

Since the mounting angle of the beam axis in the vertical plane is located not so far from nadir (at a straight flight), the circle flight with a small roll should be carried out to provide the azimuth NRCS curve measurement in the range of middle incidence angles.

The algorithm and method proposed in the paper can be used for the DNS enhancement, for designing an airborne radar system for operational measurement of the sea roughness characteristics. They are particularly important for ensuring safe landing of amphibian aircraft on the water surface, for example under search and rescue missions or fire fighting in the coastal areas and fire risk regions.

REFERENCES

Carswell, J.R.; Carson, S.C.; McIntosh, R.E.; Li, F.K.; Neumann, G.; McLaughlin, D.J.; Wilkerson, J.C; Black, P.G. and Nghiem, S.V., 1994. Airborne scatterometers: Investigating ocean backscatter under low- and high-wind conditions. *Proc. IEEE*, 82(12), pp. 1835-1860.

Chelton, D.B. and McCabe, P.J., 1985. A review of satellite altimeter measurement of sea surface wind speed: With a proposed new algorithm. *J. Geophys. Res.*, 90(C3), pp. 4707-4720.

Davydov, P.S.; Zhavoronkov, V.P.; Kashcheyev, G.V.; Krinitsyn, V.V.; Uvarov, V.S. and Khresin, I.N., 1977. *Radar Systems of Flying Apparatuses*. Transport, Moscow, USSR, 352 p., in Russian.

Feindt, F.; Wismann, V.; Alpers W. and Keller, W.C., 1986. Airborne measurements of the ocean radar cross section at 5.3 GHz as a function of wind speed. *Radio Science*, 21(5), pp. 845-856.

Hildebrand, P.H., 1994. Estimation of sea-surface wind using backscatter cross-section measurements from airborne research weather radar. *IEEE Trans. Geosci. Remote Sens.*, 32(1) pp. 110-117.

Kayton, M. and Fried, W.R., 1997. *Avionics Navigation Systems*. John Wieley & Sons, New York, USA, 773 p.

Kolchinskiy, V.Ye.; Mandurovskiy, I.A. and Konstantinovskiy, M.I., 1975. *Autonomous Doppler Facilities and Systems for Navigation of Flying Apparatuses*. Sovetskoye Radio, Moscow, USSR, 432 p., in Russian.

Long, D.G.; Donelan, M.A.; Freilich, M.H.; Graber, H.C.; Masuko, H.; Pierson, W.J.; Plant, W.J.; Weissman, D. and Wentz, F., 1996. Current progress in Ku-band model functions. Tech. Rep. MERS 96-002, Brigham Young Univ., USA, 88 p.

Mamayev, V.Ya.; Sinyakov, A.N.; Petrov, K.K. and Gorbunov, D.A., 2002. *Air navigation and elements of navigation calculations*. GUAP, Saint Petersburg, Russia, 256 p., in Russian.

Masuko, H.; Okamoto, K.; Shimada M. and Niwa, S., 1986. Measurement of microwave backscattering signatures of the ocean surface using X band and Ka band airborne scatterometers. *J. Geophys. Res.*, 91(C11), pp. 13065-13083.

Melnik, Yu.A., 1980. *Radar Methods of the Earth Exploration*. Sovetskoye Radio, Moscow, USSR, 264 p., in Russian.

Moore, R.K. and Fung, A.K., 1979. Radar determination of winds at sea. *Proc. IEEE*, 67(11), pp. 1504-1521.

Nekrasov, A., 2005a. On possibility to measure the sea surface wind vector by the Doppler navigation system of flying apparatus. *Proc. RADAR 2005*, Arlington, Virginia, USA, pp. 747-752.

Nekrasov, A., 2005b. Measuring the sea surface wind vector by the Doppler navigation system of flying apparatus having the track-stabilized four-beam Antenna. *Proc. APMC 2005*, Suzhou, China, Vol. 1, pp. 645-647.

Ouchi, K., 2000. A theory on the distribution function of backscatter radar cross section from ocean waves of individual wavelength. *IEEE Trans. Geosci. Remote Sens.*, 38(2) pp. 811-822.

Sosnovskiy, A.A. and Khaymovich, I.A., 1987. *Radio-Electronic Equipment of Flying Apparatuses*. Transport, Moscow, USSR, 256 p., in Russian.

Wismann, V., 1989. Messung der Windgeschwindigkeit über dem Meer mit einem flugzeuggetragenen 5.3 GHz Scatterometer, Dissertation zur Erlangung des Grades eines Doktors der Naturwissenschaften. Universität Bremen, Bremen, Germany, 119 S.

ACKNOWLEDGEMENTS

I would like to express my sincere thanks to Prof. Dr. Carlo Ferrari, Prof. Dr. Renata Archetti, the Interdepartmental Center of Research in Environmental Sciences, and the University of Bologna for their research opportunity provided, and to the Triple I Consortium for its a postdoctoral grant in the framework of the European Community Mobility Program Erasmus Mundus External Cooperation Window.